Sudden death of particle-pair Bloch oscillation and unidirectional propagation in a one-dimensional driven optical lattice

S. Lin,[1] X. Z. Zhang,[2] and Z. Song[1,*]
[1]*School of Physics, Nankai University, Tianjin 300071, China*
[2]*College of Physics and Materials Science, Tianjin Normal University, Tianjin 300387, China*
(Received 8 July 2014; published 2 December 2014)

We study the dynamics of bound pairs in the extended Hubbard model driven by a linear external field. It is shown that two interacting bosons or singlet fermions with nonzero on-site and nearest-neighbor interaction strengths can always form bound pairs in the absence of an external field. There are two bands of bound pairs, one of which may have incomplete wave vectors when it has an overlap with the scattering band, referred to as an imperfect band. In the presence of the external field, the dynamics of the bound pair in the perfect band exhibits distinct Bloch-Zener oscillation (BZO), while in the imperfect band the oscillation presents a sudden death. The pair becomes uncorrelated after the sudden death and the BZO never comes back. Such dynamical behaviors are robust even for the weak-coupling regime and thus can be used to characterize the phase diagram of the bound states.

DOI: 10.1103/PhysRevA.90.063411 PACS number(s): 37.10.Jk, 03.65.Ge, 05.30.Jp, 03.65.Nk

I. INTRODUCTION

The dynamics of particle pairs in lattice systems has received a lot of interest, due to the rapid development of experimental techniques. Ultracold atoms have turned out to be an ideal playground for testing few-particle fundamental physics since optical lattices provide clean realizations of a range of many-body Hamiltonians. This stimulates many experimental [1–3] and theoretical investigations in strongly correlated systems, which mainly focus on bound-pair formation [4–9], detection [10], dynamics [9,11–16], collisions between a single particle and a pair [17,18], and bound-pair condensate [19]. The essential physics of the proposed bound pair (BP) is that the periodic potential suppresses single-particle tunneling across the barrier, a process that would lead to decay of the pair. This situation cannot be changed in the general case when a weak linear potential is applied. Then a BP acts as a single particle, sharing single-particle dynamical features, such as Bloch oscillation (BO) and Bloch-Zener oscillation (BZO) [20–25].

The aim of this paper is to show that the nearest-neighbor (NN) interaction can not only lead to distinct BO and BZO, but also induce the sudden death of the oscillations within a Bloch period. We study the dynamics of BPs in the extended Hubbard model driven by a linear external field. It is shown that two interacting bosons or singlet fermions with nonzero on-site and nearest-neighbor interaction strengths can always form BPs in the absence of an external field. There are two kinds of BP, which form two bound bands. We find that the existence of the nearest-neighbor interaction can lead to overlap between the scattering band of a single particle and the bound band, which can spoil the completeness of the bound band, referred to as an imperfect band. In the presence of an external field, the dynamics of the BP in the perfect band exhibits perfect BO and BZO, while in the imperfect band the oscillation presents a sudden death. The pair becomes uncorrelated after the sudden death of the oscillation and the correlation never comes back. This behavior is of interest in both fundamental and application aspects. It can be utilized to control the unidirectional propagation of the BP wave packet by imposing a single pulse, which is of great interest for applications in cold-atom physics. Numerical simulations have shown that this scheme achieves very high efficiency and a wide spectral band. Such a unidirectional filter for a cold-atom pair may be realized in a shaking optical lattice in experiment.

This paper is organized as follows. In Sec. II, we present the model Hamiltonian, and the two-particle band structures. In Sec. III, we investigate the BP dynamics in the presence of a linear field. Section IV is devoted to the application of our finding, the realization of unidirectional propagation induced by a pulsed field. Finally, we give a summary and discussion in Sec. V.

II. MODEL HAMILTONIAN AND BAND STRUCTURE

We consider an extended Hubbard model describing interacting particles in the lowest Bloch band of a one-dimensional lattice driven by an external force, which can be employed to describe ultracold atoms or molecules with magnetic or electric dipole-dipole interactions in optical lattices. We focus on the dynamics of the BP states. The pair can be two identical bosons, or equivalently, spin-1/2 fermions in the singlet state. For simplicity we will consider only bosonic systems, but it is straightforward to extend the conclusion to singlet fermionic pairs. We consider the Hamiltonian

$$H = H_0 + F\sum_{j=1} j n_j, \tag{1}$$

where the second term describes the linear external field while H_0 is the one-dimensional Hamiltonian for the extended Bose-Hubbard model on an N-site lattice,

$$H_0 = -\kappa\sum_{j=1}(a_j^\dagger a_{j+1} + \text{H.c.}) + \frac{U}{2}\sum_{j=1} n_j(n_j-1) + V\sum_{j=1} n_j n_{j+1}. \tag{2}$$

*songtc@nankai.edu.cn

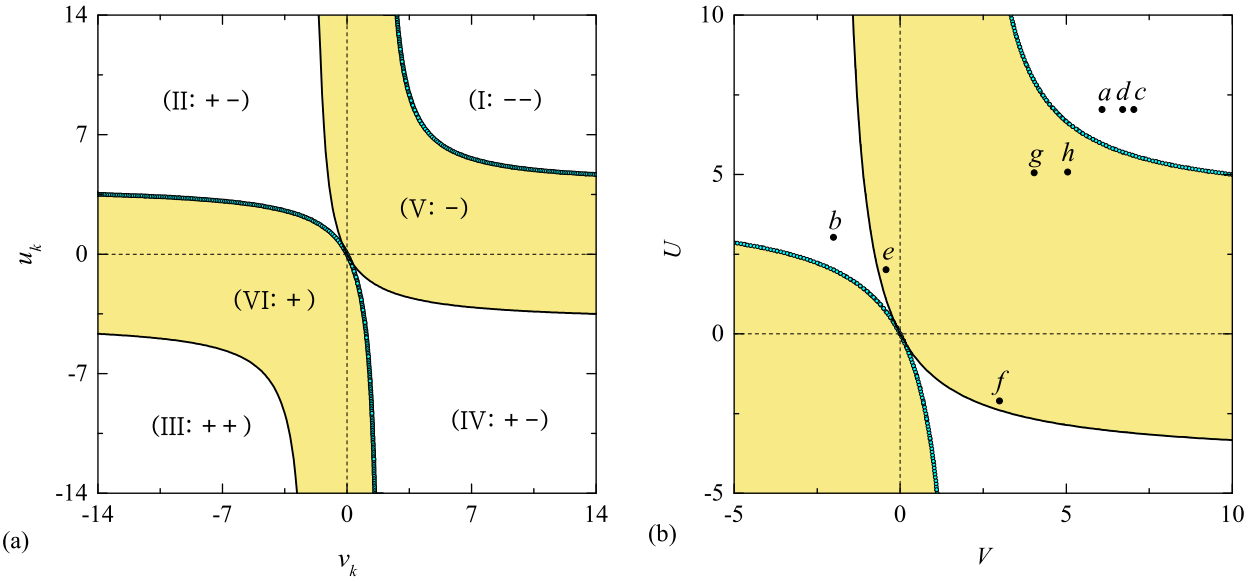

FIG. 1. (Color online) (a) Phase diagram for the BP states. The solid black (blue) line is the hyperbolic function in Eq. (10), which is the boundary of the transition from the BP state $|\psi_k^+\rangle$ ($|\psi_k^-\rangle$) to a scattering state in each invariant subspace indexed by k. There are six regions divided by the lines from Eq. (10), where $\pm$ indicates the types of bound states $|\psi_k^\pm\rangle$ in each region. (b) Phase diagram (in units of κ) indicates the features of the BP band: complete bands in regions I–IV, and incomplete bands in regions V and VI. Points $a(7,6)$, $b(3,-2)$, $c(7,7)$, $d(7,6.7)$, $e(2,-0.6)$, $f(-2,3)$, $g(5,4)$, and $h(5,5)$ denote typical cases in each phase. The band structures and dynamical features in these cases are presented in Figs. 2 and 3.

Here $a_i^\dagger$ is the creation operator of the boson at the ith site, and the tunneling strength and on-site and NN interactions between bosons are denoted by κ, U, and V.

Let us start by analyzing in detail the two-boson problem in this model. As in Refs. [15,17,18], a state in the two-particle Hilbert space can be expanded in the basis set $\{|\phi_r^k\rangle, r = 0,1,2,\ldots\}$, with

$$|\phi_0^k\rangle = \frac{1}{\sqrt{2N}}\sum_j e^{ikj}(a_j^\dagger)^2|\text{vac}\rangle, \tag{3}$$

$$|\phi_r^k\rangle = \frac{1}{\sqrt{N}}e^{ikr/2}\sum_j e^{ikj}a_j^\dagger a_{j+r}^\dagger|\text{vac}\rangle, \tag{4}$$

where $|\text{vac}\rangle$ is the vacuum state for the boson operator a_i. Here k denotes the momentum, and r is the distance between the two particles. Due to the translational symmetry of the present system, we have the following equivalent Hamiltonian:

$$H_{\text{eq}}^k = -J_k\left(\sqrt{2}|\phi_0^k\rangle\langle\phi_1^k| + \sum_{j=1}|\phi_j^k\rangle\langle\phi_{j+1}^k| + \text{H.c}\right) + U|\phi_0^k\rangle\langle\phi_0^k| + V|\phi_1^k\rangle\langle\phi_1^k| \tag{5}$$

in each invariant subspace indexed by k. In its present form, H_{eq}^k is formally analogous to the tight-binding model describing a single-particle dynamics in a semi-infinite chain with the k-dependent hopping integral $J_k = 2\kappa\cos(k/2)$ in the thermodynamic limit $N \to \infty$. In this paper, we are interested in the BP states, which correspond to the bound-state solution of the single-particle Schrödinger equation

$$H_{\text{eq}}^k|\psi_k\rangle = \epsilon_k|\psi_k\rangle. \tag{6}$$

For a given J_k, the Hamiltonian H_{eq}^k possesses one or two bound states, which are denoted as $|\psi_k^+\rangle$ and $|\psi_k^-\rangle$, respectively. Here the Bethe-ansatz wave functions have the form

$$|\psi_k^\pm\rangle = C_0^k|\phi_0^k\rangle + \sum_{r=1}(\pm 1)^r C_r^k e^{-\beta r}|\phi_r^k\rangle, \tag{7}$$

with $\beta > 0$. For two such bound states $|\psi_k^\pm\rangle$ the Schrodinger equation in Eq. (6) admits

$$\pm e^{3\beta} + (u_k + v_k)e^{2\beta} \pm (u_k v_k - 1)e^\beta + v_k = 0, \tag{8}$$

where $u_k = U/J_k$ and $v_k = V/J_k$ are respectively the reduced interaction strengths. The corresponding bound-state energy of $|\psi_k^\pm\rangle$ can be expressed as

$$\epsilon_k^\pm = \pm J_k\cosh\beta. \tag{9}$$

The transition from bound to scattering states occurs at $\beta = 0$. Then the boundary at which the bound state $|\psi_k^\pm\rangle$ disappears is described by the hyperbolic function

$$u_k = -\frac{2v_k}{1 \pm v_k}, \tag{10}$$

which is plotted in Fig. 1. It shows that the boundary lines divide the u_k-v_k plane into six regions, from I to VI. The type of bound states in each region can be foreseen from the extreme situations where $|u_k|, |v_k| \gg 1$. Under this condition, it is easy to check that there are two bound states with the eigenenergies

$$\epsilon_k^\pm \approx U \text{ and } V, \tag{11}$$

in each invariant k subspace. Comparing Eqs. (11) and (9), we arrive at the conclusion that there are two bound states in the regions I, II, III, and IV: two $|\psi_k^-\rangle$ in I, one $|\psi_k^+\rangle$ and $|\psi_k^-\rangle$

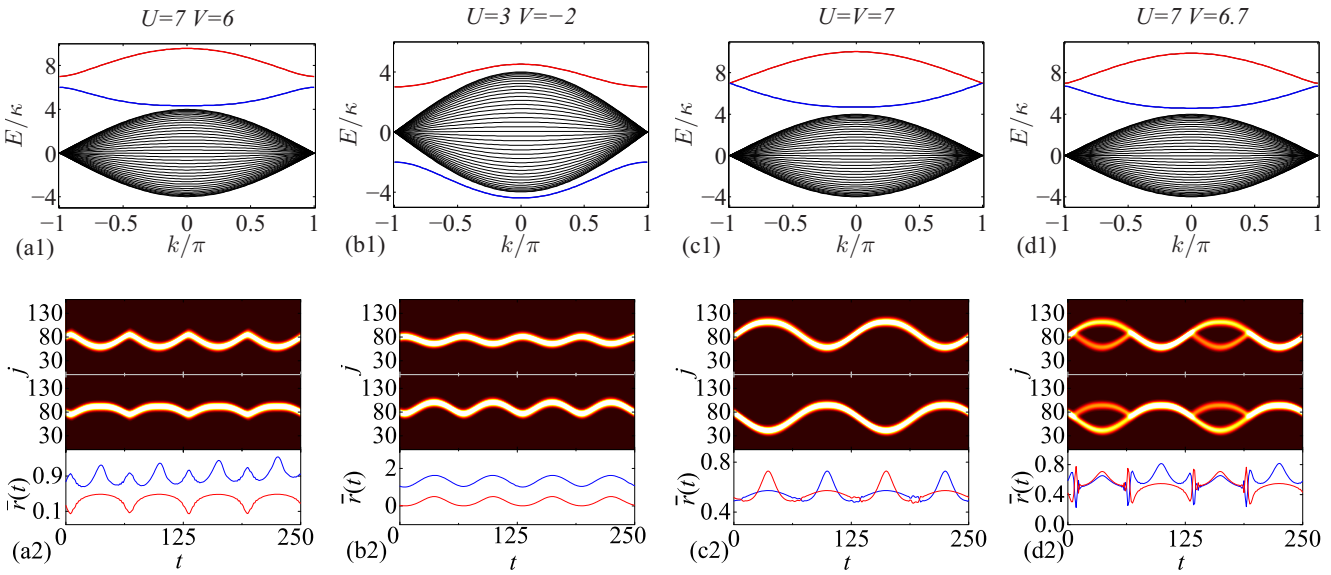

FIG. 2. (Color online) (a1)–(d1) The band structures for the systems with parameters fixed at the typical points (*a*-*d*) labeled in Fig. 1. All the BP bands are complete. (a2)–(d2) The profiles and the average distances $\bar{r}(t)$ of the time evolution of the initial wave packets in the form of Eq. (19) with $k_0 = -0.8\pi$, $\alpha = 0.15$, and $N_A = 80$ of the two BP bands, in an external field with $F_0 = 0.05$, in which the time t is expressed in units of $1/\kappa$. We can see the perfect BO and BZO phenomena. The evolution of $\bar{r}(t)$ shows that the correlation of the BP remains strong.

in II and IV, and two $|\psi_k^+\rangle$ in III, while there are bound states $|\psi_k^-\rangle$ in V and $|\psi_k^+\rangle$ in VI, respectively.

On the other hand, we know that the scattering band of $H_{\rm eq}^k$ ranges from $-4\kappa\cos(k/2)$ to $4\kappa\cos(k/2)$, which reaches the widest bandwidth at $k = 0$. Therefore, when we take $J_0 = \pm 2\kappa$, this diagram can characterize the bound-state number distribution $N_b(U,V)$: we have $N_b = 2N$ in the regions I, II, III, and IV, where all the $2N$ bound states indexed by k constitute a complete BP band. In contrast, we have $N_b < 2N$ in V and VI, where all N_b bound states are indexed by the survival k, which does not cover the whole range of momentum in the Brillouin zone, from $-\pi$ to π. We refer to this property as an incomplete BP band. Therefore, the phase diagram also indicates the boundary $U = -2V/(1 \pm V)$, for the transition from the complete to the incomplete BP bands, which agrees with the results reported in Refs. [6,26,27]. For given U and V, the complete spectrum of H_0 can be computed by diagonalizing the Hamiltonian $H_{\rm eq}^k$ numerically. In Figs. 2 and 3, we plot the band structures for several typical cases, which are marked in Fig. 1. We do not cover all the typical points in every region due to the following fact. The spectrum of H_0 obeys the relation

$$E_k(U,V) = -E_k(-U,-V), \tag{12}$$

in view of

$$H_0(U,V) = -RH_0(-U,-V)R^{-1}, \tag{13}$$

where the transformation R is defined as $Ra_jR^{-1} = (-1)^j a_j$. It is a rigorous result in the whole range of the parameters. As expected, we observe that the two-particle spectrum comprises three Bloch bands, two BP bands formed by two kinds of BP states, and one scattering band formed by uncorrelated states. We can see from Fig. 2 that two bound bands are separated from the scattering band whenever the system is in the regions I, II, III, and IV (points a, b, c, and d). In contrast, whenever the points (e, f, g, and h) lie in the regions V and VI, the pseudogap between the BP and the scattering bands around $k = 0$ vanishes, resulting in the formation of an incomplete band. What is quite unexpected and remarkable is that if we apply a linear field, the dynamics of the BP exhibits some peculiar behaviors, which will be investigated in the following section.

III. BP DYNAMICS

Before starting the investigation of the BP dynamics, we would like to study the relation between the center path of a wave packet driven by a linear field and dispersion of the Hamiltonian H_0. Consider a general one-dimensional tight-binding system, which has the dispersion relation $E(k)$ that is an arbitrary smooth periodic function $E(2\pi + k) = E(k)$. The dynamics of the wave packet can be simply understood in terms of a semiclassical picture: A wave packet centered around k_c can be regarded as a classical particle with momentum k_c [28–30]. When the wave packet is subjected to a homogeneous force of strength F, the acceleration theorem $\partial k_c(t)/\partial t = F$ tells us that

$$\begin{aligned} k_c(t) &= k_c(0) + \int_0^t F dt \\ &= k_c(0) + Ft \end{aligned} \tag{14}$$

for a constant field. The central position of the wave packet is

$$\begin{aligned} x_c(t) &= x_c(0) + \int_0^t v_g dt \\ &= x_c(0) + \frac{1}{F}[E_k(k_c(0) + Ft) - E_k(k_c(0))] \end{aligned} \tag{15}$$

where $v_g = \partial E_k/\partial k$ is the group velocity. Notice that the trajectory of a wave packet is essentially identical with the dispersion relation for the field-free system under the

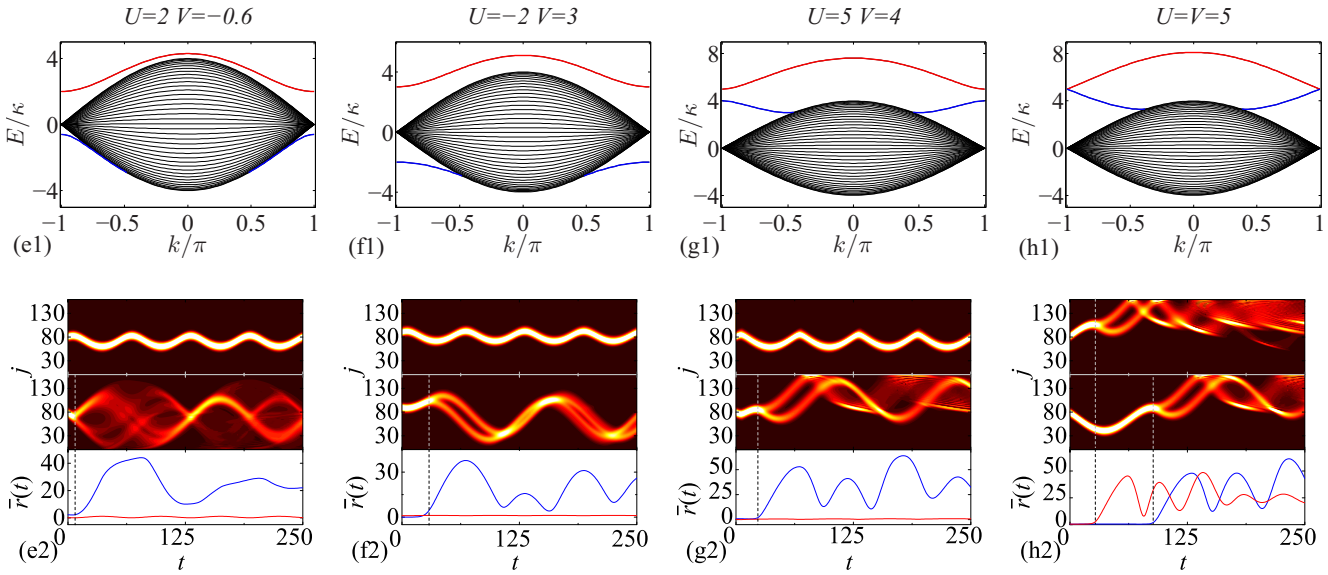

FIG. 3. (Color online) As Fig. 2 but for systems with parameters fixed at the typical points e–f labeled in Fig. 1. It shows that the BP band becomes incomplete due to the overlap between the bound and scattering energy levels. We can see the sudden death of the BO, which closely accompanies the breakdown of the pair correlation. Here the time t is also expressed in units of $1/\kappa$.

semiclassical approximation. This observation provides a fairly clear picture of the dynamics of a wave packet in the presence of a linear field. As a simple example we consider the single-particle case for illustration. The single-particle BO with Bloch frequency $\omega_B = F$ for H can be simply understood from its cosinusoidal dispersion relation $E(k) = -2\kappa \cos k$, rather than quadratic, in momentum k.

Now, we switch gears to the case of two particles. We note that the bandwidth of the BP band is comparable to that of the scattering band, which leads to the conclusion that a BP wave packet has a distinct group velocity. This indicates that the dynamics of the BP state has similar behavior to that of the single particle. The BO-like behavior of the BP wave packet emerges in the presence of a linear external field.

In order to demonstrate these points, we consider an example for the Hamiltonian H in Eq. (1) with $U, V \gg |U - V|\kappa$. As studied in Ref. [15], in the absence of the external field, the BP lies in the quasi-invariant subspace spanned by the basis $\{|\underline{l}\rangle\}$, which is defined as

$$|\underline{l}\rangle \equiv \begin{cases} (a^\dagger_{l/2})^2/\sqrt{2}|\text{vac}\rangle & (\text{even } l), \\ a^\dagger_{(l-1)/2} a^\dagger_{(l+1)/2}|\text{vac}\rangle & (\text{odd } l). \end{cases} \tag{16}$$

In the presence of the external field, the bound pair can be described by the following effective Hamiltonian:

$$H_{\text{eff}} = -\sqrt{2}\kappa \sum_l (|\underline{l}\rangle\langle \underline{l+1}| + \text{H.c.}) + \sum_l \left[Fl + \frac{\delta}{2}(-1)^l \right] |\underline{l}\rangle\langle \underline{l}|, \tag{17}$$

where we neglect a constant term $(U + V)/2 \sum_l |\underline{l}\rangle\langle \underline{l}|$ and take $\delta = U - V$ to represent the unbalanced on-site and nearest-neighbor interactions. H_{eff} is nothing but the tight-binding Hamiltonian that describes a single particle subjected to a staggered linear potential, which has been well studied in previous literature [31]. Unlike the fractional BO [32–35] in the case of $V = 0$, H_{eff} can support a wide bandwidth [15], which is responsible for the large-amplitude oscillations. In the situation with $\delta = 0$, it turns out that the particle undergoes a BO with frequency $\omega_B = F$. In the case of nonzero imbalance $\delta \neq 0$, it has been reported that the dynamics of the wave packet shows a BZO, a coherent superposition of Bloch oscillations and Zener tunneling between the sub-bands. The Zener tunneling takes place almost exclusively when the momentum of the wave packet reaches $\pm\pi$. Then we arrive at the conclusion that the BPs serve as composite particles, exhibiting BO and BZO in the strong-coupling region.

In this paper we are interested in what happens if the initial state is placed in an incomplete band. We presume that the semiclassical theory still holds when the wave packet is inside the extent of the incomplete band, because the nonzero pseudogap can protect the BP wave packet from the scattering band. However, when the wave packet reaches the band edge, the transition from the bound to the scattering band occurs. The wave packet diffuses into the continuous spectrum rather than undergoing the repetitive motion of acceleration and Bragg reflection. We refer to this phenomenon as the sudden death of the BO. In the case of the incomplete BP band with an edge $k_m > 0$, the lifetime τ for an initial wave packet with $k_c(0)$ satisfies

$$k_m = |k_c(0) + \tau F|. \tag{18}$$

When this occurs, the correlation between the two particles breaks down and the wave packet spreads out in space, irreversibly.

To verify and demonstrate the above analysis, numerical simulations are performed to investigate the dynamics behavior. We compute the time evolution of the wave packet by diagonalizing the Hamiltonian H numerically. Throughout this paper, we investigate the dynamics of the initial Gaussian

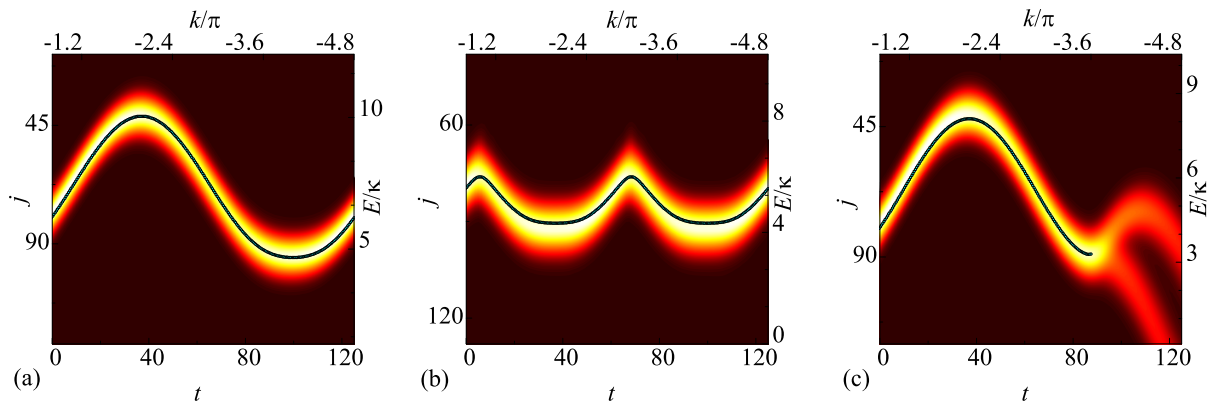

FIG. 4. (Color online) The comparison between the BP dispersion relations and the central positions for the cases plotted in Figs. 2 and 3: (a) lower band in c; (b) lower band in a; (c) lower band in h. This shows that the two are in close proximity to each other even for the case of the incomplete band, which corresponds to the sudden death of the BO. The time t is expressed in units of $1/\kappa$.

wave packet in the form

$$|\Psi(0)\rangle = \Lambda \sum_k \exp\left[-\frac{(k-k_0)^2}{2\alpha^2} - iN_A(k-k_0)\right]|\psi_k\rangle, \tag{19}$$

where Λ is a normalization factor, and k_0 and N_A denote the central momentum and position of the initial wave packet, respectively. The evolved state under the Hamiltonian H is $|\Psi(t)\rangle = e^{-iHt}|\Psi(0)\rangle$. We would like to stress that the initial wave packet involves one BP band, either the upper or the lower one. However, the evolved state may involve two BP bands, even the scattering band, when Zener tunneling occurs. We plot the probability profile of the wave packet evolution in several typical cases in Figs. 2 and 3. In Fig. 2, the simulation is performed in systems where the two bound bands are well separated from the scattering band. As the external field is turned on, several dynamical behaviors occur: when the two bound bands are well separated (a1) and (b1), BOs in both bands are observed (a2) and (b2). In the case (d1),(d2), two bound bands are very close at $\pm\pi$, which induces the BZO as expected. For these three cases, the BO frequency doubles compared with that of the single-particle case. The case (c1),(c2) fixes $U = V$, two bound bands merge into a single bound band. As predicted above, simple BO rather than BZO is observed, with a period equal to that of single-particle BO. In Fig. 3, the systems have a common feature: one of the BP bands is incomplete due to the pseudogap vanishing. In the three cases (e2), (f2), and (g2), the BOs remain in one band, whereas the BOs break down at the edges of the incomplete band. For the cases (h1),(h2) with $U = V$, two bound bands merge into a single incomplete band. The BP wave packets in both bands cannot survive because of the irreversible spreading.

Furthermore, the correlation between the two particles is measured by the average distance between the two particles,

$$\bar{r}(t) = \sum_{i,r} r\langle\Psi(t)|n_i n_{i+r}|\Psi(t)\rangle, \tag{20}$$

which can be used to characterize the feature of sudden death of BO for an evolved state $|\Psi(t)\rangle$. As comparison, the average distance $\bar{r}(t)$ as a function of time for several typical cases is plotted in Figs. 2 and 3. We find that the sudden death of BO is always accompanied by the irreversible increase of $\bar{r}(t)$, which accords with our analytical predictions.

Finally, we also plot the BP dispersion relation $E(k)$ and the central position $x_c(t)$ of the wave packet under the driving force together in one figure. For several typical cases, the plots in Fig. 4 indicate that the shape of the function $x_c(t)$ coincides with that of the dispersion relation $E(k)$. We also find that the semiclassical analysis in Eq. (15) is valid if δ is not too small. Remarkably, one can see that such a relation still holds even for the incomplete BP band. These results are in agreement with the theoretical prediction based on the spectral structures.

IV. UNIDIRECTIONAL PROPAGATION

We now investigate the effect of the a time-dependent driving force on the dynamics of a BP wave packet. The acceleration theorem (14) tells us that a pulsed field can shift the central momentum of the wave packet in the case of the complete band. However, it is easy to find that a pulsed field may destroy a BP wave packet in the incomplete band, similarly referred to as the sudden death of uniform motion. The death and survival of a propagating wave packet strongly depend on the difference between the initial central momentum and the edge of the incomplete band. Of course, a surviving wave packet can be caused to retain its original state of motion by a subsequently compensating pulsed field. This gives rise to a scheme for destroying the pair wave packet propagating in one direction, but retaining the one with the opposite direction. This kind of scheme can be carried out by two pulsed fields in a pair of adjacent intervals, which provides two opposite impulses to the wave packet (see Fig. 5).

To illustrate the scheme, we propose two concrete examples. The first one is a square-wave pulse driving force in the form

$$F(t) = \begin{cases} F_0, & -T/2 < t \leqslant 0, \\ -F_0, & 0 < t \leqslant T/2, \\ 0 & \text{otherwise.} \end{cases} \tag{21}$$

According to the acceleration theorem, an initial wave packet with momentum $k_c(0)$ will acquire a momentum shift $F_0T/2$

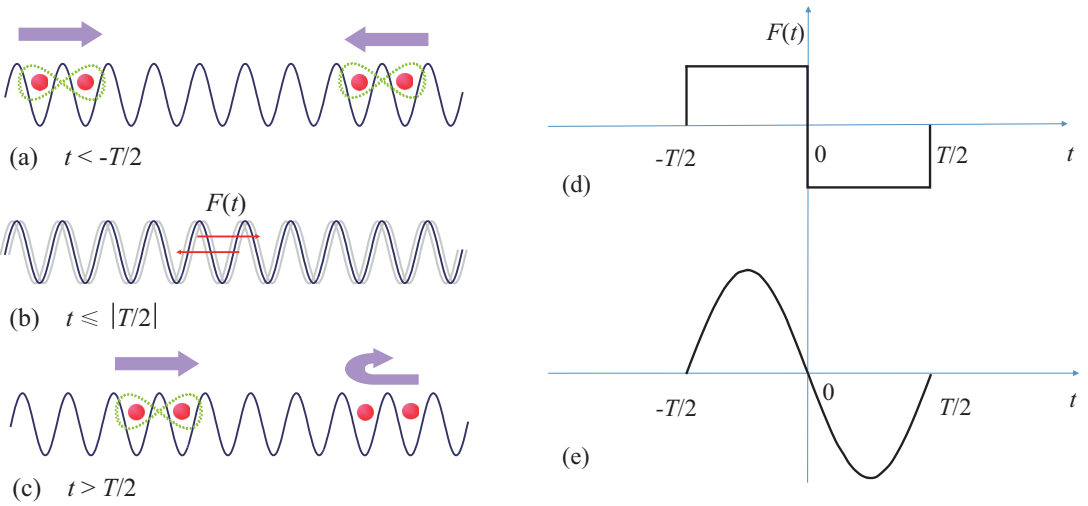

FIG. 5. (Color online) Schematic illustration for the process of realizing unidirectional propagation of the BP. The dashed ∞ represents the correlation between the two particles. The shaking lattice induces an inertial force $F(t)$. (a) For $t < -T/2$, the bound-pair wave packet moves towards the right or left with constant group velocity. (b) During the period of time $[-T/2, T/2]$, a pulsed field $F(t)$ is caused to act on the pairs by shaking the lattice back and forth, which may break down the BP moving to the left. (c) After the time $T/2$, the surviving wave packet goes back to its original state, while another pair is bounded back and becomes uncorrelated. (d) and (e) are two example forms of $F(t)$, which are taken for the numerical simulations in Fig. 6.

at the instant $t = 0$ if $k_c(0) + F_0 T/2$ is within the band. The action of the subsequent force $-F_0$ can return the group velocity to its initial value, continuing its motion in the same direction. However, in the case of $k_c(0) + F_0 T/2$ beyond the incomplete band, the BP wave packet breaks down before $t = 0$ and the subsequent force cannot regain the correlation. Therefore, for two BP wave ackets with opposite momenta $\pm k_c(0)$ or group velocities $\pm v_g(0)$, one can always choose a proper $F(t)$ to destroy one of them and maintain the other. This feature can be used to control the direction of wave packet propagation on demand. Alternatively, one can also consider a sine-wave pulse driving force

$$F(t) = \begin{cases} (-F_0\pi/2)\sin(2\pi t/T), & t \leqslant |T/2|, \\ 0 & \text{otherwise}, \end{cases} \tag{22}$$

to achieve the same effect as from Eq. (14). To examine how these schemes work in practice, we apply them to a wave packet in the form of (19). Figure 6 shows a numerical propagation of the Gaussian wave packet under the action of two kinds of pulsed driving forces. It shows that wave

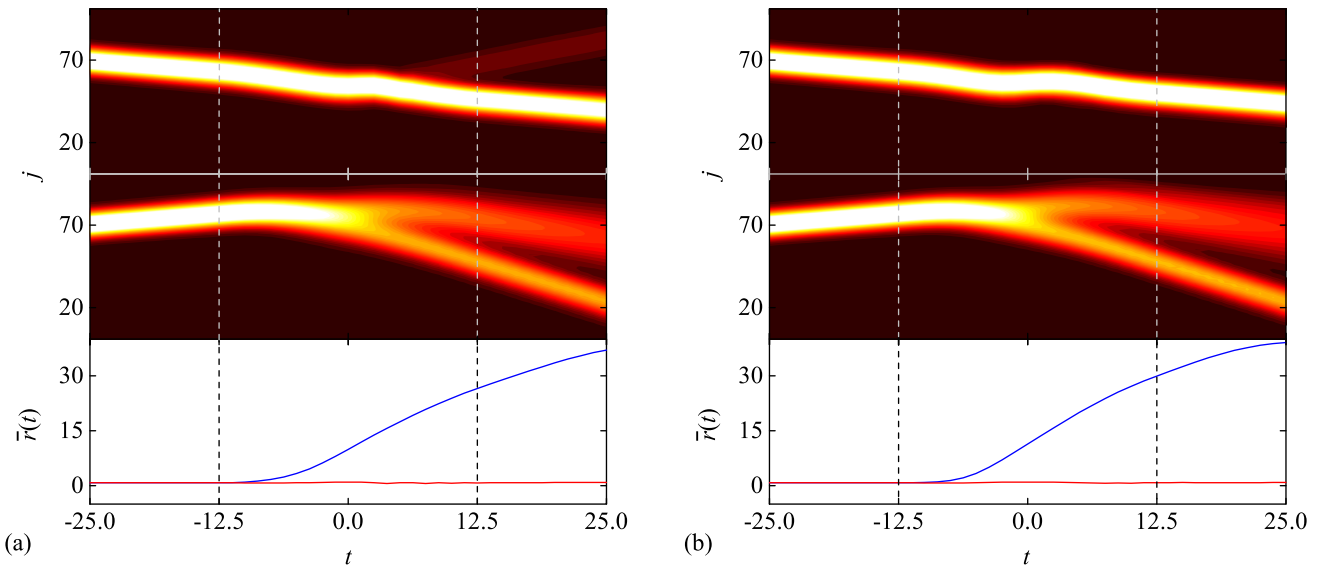

FIG. 6. (Color online) The profiles and the avarage distances $\bar{r}(t)$ of the time evolution of the initial wave packets in the form of Eq. (19) with $k_0 = \pm 0.6\pi$, $\alpha = 0.15$, and $N_A = 70$, in the lower band of the system with $U = 5$, $V = 4$, and $F_0 = 0.05$. The pulsed field is taken in the forms of (a) a square wave and (b) a sine wave, respectively. We can see in both cases that the wave packet with $k_0 = -0.6\pi$ is spread out by the pulse field, while the one with $k_0 = 0.6\pi$ remains in its original state of motion. Here the time t is expressed in units of $1/\kappa$.

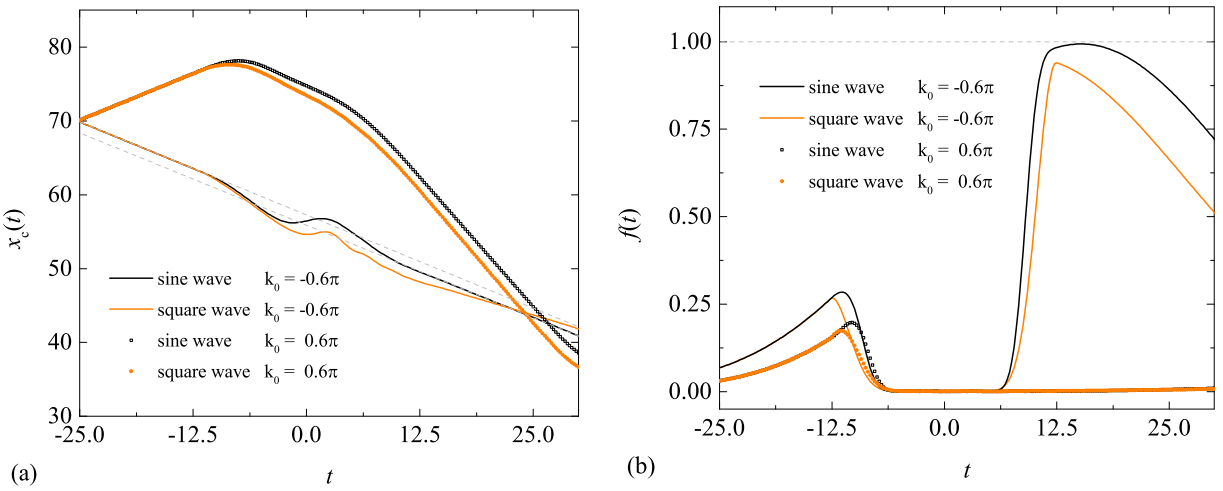

FIG. 7. (Color online) Plots of the c.m. $x_c(t)$ (a) and the fidelity $f(t)$ (b) for the process illustrated in Fig. 6, where the time t is expressed in units of $1/\kappa$. (a) clearly shows that the pulsed field bounces back one pair but maintains the other. The gray dashed lines are drawn as guidance to the eye, indicating the initial and final paths for the case of a sine wave. (b) indicates that the sine-wave pulse has very high efficiency for the control of unidirectional propagation.

packets with opposite group velocities exhibit entirely different behaviors: one remains in the original state of motion, while the other spreads out in space. Remarkably, the probability of the broken wave packet is reflected by the pulsed field, which indicates that the unidirectional effect in the scheme works not only for the two-particle correlation but also for the probability flow. In addition, one can see a slight separation from the moving wave packet under the action of the square-wave pulsed field. The probability flow of two particles, no matter whether correlated or not, can be depicted by the center of mass (c.m.)

$$x_c(t) = \sum_j \langle j n_j \rangle_t, \tag{23}$$

where $\langle \cdots \rangle_t$ denotes the average for the evolved state. On the other hand, to characterize the efficiency of the schemes, we introduce the fidelity defined as

$$\begin{aligned} \mathcal{F} &= \max[f(t)], \\ f(t) &= |\langle \Psi_t(t) | \Psi_0(t_0) \rangle|, \end{aligned} \tag{24}$$

where

$$|\Psi_0(t_0)\rangle = \exp(-i H_0 t_0) |\Psi(0)\rangle \tag{25}$$

is the target state and

$$|\Psi_t(t)\rangle = \mathcal{T} \exp\left(-i \int_0^t H(t) dt\right) |\Psi(0)\rangle \tag{26}$$

is the transferred state subjected to a pulsed field. Here we have omitted a shift on the time scale compared to the expression of $F(t)$. The computation is performed by using a uniform mesh in the time discretization for the time-dependent Hamiltonian $H(t)$. As an example, in Fig. 7, we show the evolution of the c.m. $x_c(t)$ and the fidelity $f(t)$ for the same parameter values as the four processes simulated in Fig. 6. The plot in (a) shows the behavior of the two-particle transmission and reflection induced by the pulsed field, while in (b) the fidelities of the state are transferred. It indicates that a sine-wave pulse has a higher fidelity ($\mathcal{F} = 0.994$) than that of square-wave pulse ($\mathcal{F} = 0.940$). These results clearly demonstrate the power of the mechanism proposed in this paper with the purpose of inducing unidirectional propagation which is caused by a pulsed field.

It is easy to estimate the spectral band of the unidirectional filter by neglecting the width of the wave packet. We find that there are three reasons that trigger the death of a propagating wave packet: (i) the central momentum of the initial wave packet, (ii) the edge of the incomplete band, which is determined by the values of U/κ and V/κ, and (iii) the impulse of the single pulsed field. We consider a lattice with one bound band just touching the scattering band at the center momentum $k = 0$. We note, but do not prove exactly, that the dispersion relations in the left region $[-\pi,0]$ and right region $[0,\pi]$ are monotone functions. Then if we apply a pulsed field with impulse π, a moving wave packet with momentum in the left region should be pushed into the scattering band and will not be recovered by the subsequent $-\pi$ impulse. In contrast, a wave packet in the right region still keep its initial situation after this process. Therefore, roughly speaking, the proposed unidirectional filter works for wave packets with all possible group velocities.

V. SUMMARY

In this paper, the coherent dynamics of two correlated particles in the one-dimensional extended Hubbard model with on-site U and nearest-neighbor site V interactions, driven by a linear field, has been theoretically investigated. The analysis shows that in the free-field case, there always exist BP states for any nonzero U and V, which may have comparable bandwidth with that of single particle. This results in the onset of distinct BO and BZO for a correlated pair in the presence of an external field. We found that the incompleteness of the BP band spoils the correlation of the pair and leads to the sudden death of the BO and BZO. Based on this mechanism, we propose a scheme to control the unidirectional propagation of the BP wave packet

by imposing a single pulse. As a simple application of this scheme, we investigate the effects of two kinds of pulsed field. Numerical simulations indicate that a sine-wave pulse has a higher fidelity than that of a square-wave pulse. In experiment, it has been proposed that ultracold atomic gases in optical lattices with sinusoidal shaking can be an attractive testing ground to explore the dynamical control of quantum states [36–39]. The sudden death of BO predicted in this paper is an exclusive signature of a correlated particle pair and could be applied to quantum and optical device design.

ACKNOWLEDGMENTS

We acknowledge the support of the National Basic Research Program (973 Program) of China under Grant No. 2012CB921900 and CNSF (Grant No. 11374163).

[1] K. Winkler, G. Thalhammer, F. Lang, R. Grimm, J. H. Denschlag, A. J. Daley, A. Kantian, H. P. Büchler, and P. Zoller, Nature (London) **441**, 853 (2006).
[2] S. Fölling, S. Trotzky, P. Cheinet, M. Feld, R. Saers, A. Widera, T. Müller, and I. Bloch, Nature (London) **448**, 1029 (2007).
[3] M. Gustavsson, E. Haller, M. J. Mark, J. G. Danzl, G. Rojas-Kopeinig, and H. C. Nägerl, Phys. Rev. Lett. **100**, 080404 (2008).
[4] S. M. Mahajan and A. Thyagaraja, J. Phys. A **39**, L667 (2006).
[5] M. Valiente and D. Petrosyan, J. Phys. B **41**, 161002 (2008).
[6] M. Valiente and D. Petrosyan, J. Phys. B **42**, 121001 (2009).
[7] M. Valiente, D. Petrosyan, and A. Saenz, Phys. Rev. A **81**, 011601(R) (2010).
[8] J. Javanainen, O. Odong, and J. C. Sanders, Phys. Rev. A **81**, 043609 (2010).
[9] Y. M. Wang and J. Q. Liang, Phys. Rev. A **81**, 045601 (2010).
[10] A. Kuklov and H. Moritz, Phys. Rev. A **75**, 013616 (2007).
[11] D. Petrosyan, B. Schmidt, J. R. Anglin, and M. Fleischhauer, Phys. Rev. A **76**, 033606 (2007).
[12] S. Zöllner, H.-D. Meyer, and P. Schmelcher, Phys. Rev. Lett. **100**, 040401 (2008).
[13] L. Wang, Y. Hao, and S. Chen, Eur. Phys. J. D **48**, 229 (2008).
[14] M. Valiente and D. Petrosyan, Europhys. Lett. **83**, 30007 (2008).
[15] L. Jin and Z. Song, New J. Phys. **13**, 063009 (2011).
[16] G. Corrielli, A. Crespi, G. D. Valle, S. Longhi, and R. Osellame, Nat. Commun. **4**, 1555 (2012).
[17] L. Jin, B. Chen, and Z. Song, Phys. Rev. A **79**, 032108 (2009).
[18] L. Jin and Z. Song, Phys. Rev. A **81**, 022107 (2010).
[19] A. Rosch, D. Rasch, B. Binz, and M. Vojta, Phys. Rev. Lett. **101**, 265301 (2008).
[20] J. G. Muga, J. P. Palao, B. Navarro, and I. L. Egusquiza, Phys. Rep. **395**, 357 (2004).
[21] L. Poladian, Phys. Rev. E **54**, 2963 (1996).
[22] M. Greenberg and M. Orenstein, Opt. Lett. **29**, 451 (2004).
[23] M. Kulishov, J. M. Laniel, N. Belanger, J. Azana, and D. V. Plant, Opt. Express **13**, 3068 (2005).
[24] A. Ruschhaupt, J. G. Muga, and M. G. Raizen, J. Phys. B **39**, 3833 (2006).
[25] S. Longhi, Phys. Rev. B **86**, 075144 (2012).
[26] W. S. Dias, M. L. Lyra, and F. A. B. F. de Moura, Phys. Lett. A **374**, 4554 (2010).
[27] R. Khomeriki, D. O. Krimer, M. Haque, and S. Flach, Phys. Rev. A **81**, 065601 (2010).
[28] F. Bloch, Z. Phys. **52**, 555 (1929).
[29] N. W. Ashcroft and N. D. Mermin, *Solid State Physics* (Harcourt, Fort Worth, TX, 1976), Chap. 12.
[30] C. Kittel, *Quantum Theory of Solids*, 2nd ed. (Wiley, New York, 1987).
[31] B. M. Breid, D. Witthaut, and H. J. Korsch, New J. Phys. **8**, 110 (2006).
[32] A. Buchleitner and A. R. Kolovsky, Phys. Rev. Lett. **91**, 253002 (2003).
[33] A. R. Kolovsky, Phys. Rev. A **70**, 015604 (2004).
[34] K. Kudo, T. Boness, and T. S. Monteiro, Phys. Rev. A **80**, 063409 (2009).
[35] K. Kudo and T. S. Monteiro, Phys. Rev. A **83**, 053627 (2011).
[36] K. W. Madison, M. C. Fischer, R. B. Diener, Q. Niu, and M. G. Raizen, Phys. Rev. Lett. **81**, 5093 (1998).
[37] N. Gemelke, E. Sarajlic, Y. Bidel, S. Hong, and S. Chu, Phys. Rev. Lett. **95**, 170404 (2005).
[38] H. Lignier, C. Sias, D. Ciampini, Y. Singh, A. Zenesini, O. Morsch, and E. Arimondo, Phys. Rev. Lett. **99**, 220403 (2007).
[39] Y. A. Chen, S. Nascimbène, M. Aidelsburger, M. Atala, S. Trotzky, and I. Bloch, Phys. Rev. Lett. **107**, 210405 (2011).